EURASIP Journal on Applied Signal Processing 2005:4, 541–549

Digital Compensation in IQ Modulator Using H_∞ Optimization—A State-Space Approach

A. G. K. C. Lim
School of Electrical, Electronic and Computer Engineering, University of Western Australia, 35 Stirling Highway, Crawley, WA 6009, Australia
Email: lim-ka@ee.uwa.edu.au

V. Sreeram
School of Electrical, Electronic and Computer Engineering, University of Western Australia, 35 Stirling Highway, Crawley, WA 6009, Australia
Email: sreeram@ee.uwa.edu.au

G. Wang
School of Electrical, Electronic and Computer Engineering, University of Western Australia, 35 Stirling Highway, Crawley, WA 6009, Australia
Email: wang-g@ee.uwa.edu.au

Received 30 April 2004; Revised 5 October 2004; Recommended for Publication by Thomas Kaiser

In DSP-based IQ modulators generating CPFSK signals, shortcomings in the implementation of the analog reconstruction filters result in the loss of the constant envelope property of the output CPFSK signal. These ripples cause undesirable spreading of the transmitted signal spectrum into adjacent channels when the signal passes through nonlinear elements in the transmission path and the consequent failure of the transmitted signal in meeting transmission standards requirements. Therefore, digital techniques compensating for these shortcomings play an important role in enhancing the performance of the IQ modulation system. Recently, several methods have been proposed in the literature to digitally compensate for the imperfections in the transfer characteristics of the analog reconstruction filters. Although these methods have been shown to be effective in removing the output envelope ripples, they result in filters of high orders and are therefore computationally demanding to implement on the DSP. Furthermore, previous techniques suffer from numerical instabilities as a result of matrix inversion in the process of calculating the solution vector. In this paper, we present two new techniques for designing the digital compensation filters by means of H_∞ optimization to address the limitations of previous solutions. Design of control systems by H_∞ optimization is now a standard technique. Simulation examples show that these techniques are effective and lead to substantial improvement of the output envelope ripples.

Keywords and phrases: H-infinity optimization, digital compensation, IQ modulators.

1. INTRODUCTION

Wireless communications are currently undergoing enormous growth and change. Much of the current development in wireless communication is based on digital communication principles. Digital subsystems are used extensively to implement radio transceivers [1]. The current trend in software-defined radios is the replacement of as much analog subsections of a radio transceiver as possible with programmable digital hardware [2]. In this paper, we consider the use of inphase/quadrature (IQ) modulation in transceiver architecture. A versatile approach to the implementation of an IQ modulator is to synthesize the base-band I and Q signals using a digital signal processor (DSP) followed by a vector modulator to upconvert the signals directly into radio-frequency (RF) signals. The IQ modulator structure incorporating DSP is shown in Figure 1. Here, the I and Q channel baseband signals are generated digitally using a DSP and converted into analog signals using digital-to-analog (D/A) converters and analog reconstruction filters before modulation and transmission.

However, the performance of such configuration can be limited by the two analog reconstruction filters (labelled LPF1 and LPF2) that are necessary to attenuate digital image components in the baseband signal spectrum before transmission. The transfer characteristics of practical reconstruction filters and errors in their implementation result in the passband characteristics departing from constant magnitude and linear phase. Furthermore, implementation errors also result in a mismatch between the I and Q channel

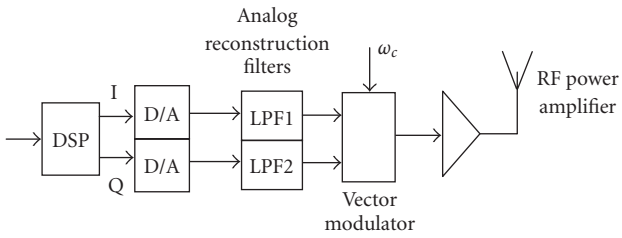

Figure 1: Radio transmitter architecture incorporating digital IQ modulation.

reconstruction filter frequency responses. In the case of continuous-phase-frequency shift Keying (CPFSK) signals, these shortcomings cause distortion of the I and Q channel signals resulting in the loss of the constant envelope property of the output CPFSK signal. This can cause significant degradation of the performance of the transmitter system. Ripples in the envelope function cause undesirable spreading of the signal spectrum into adjacent channels when the signal passes through a nonlinear RF power amplifier (PA) in the transmitter [3, 4].

Digital compensation for the shortcomings in the analog subsystems of quadrature modulators has received considerable attention in the literature lately [5, 6, 7, 8, 9]. Shortcomings in the implementation of the analog subsystems can be classified into two categories, that is, static errors and frequency-dependent transfer characteristics errors. Here, we will consider only the frequency-dependent errors. Extensive work has been done on digital predistortion techniques [3, 4], which compensate for nonlinearities in the power amplifier shown in Figure 1 in an effort to reduce spreading of the transmitted signal spectrum into adjacent frequency channels. However, most of these techniques ignore the effects of the analog reconstruction filters, and in [4] it is shown that the characteristics of the two analog lowpass filters can significantly reduce the usefulness of some of these techniques.

The principal sources of the frequency-dependent transfer characteristics errors are the two analog reconstruction filters. The study of the effect of analog reconstruction filters on the performance of the quadrature modulator has been reported in [3, 4]. Nevertheless, little work has been presented on compensating for the frequency-dependent characteristics of the analog reconstruction filters.

In [6], a method was proposed to remove the unwanted ripples at the vector modulator's output signal envelope using digital signal preshaping filters in the I and Q channels. This is to precompensate for both imbalances in the analog reconstruction filters' frequency responses as well as departures from constant magnitude, linear phase in the passband of each reconstruction filter. This method employs a *least-square* (LS) optimization approach where the precompensation finite impulse response (FIR) filters are found by minimizing the *least-square* error of the error transfer function. An alternative solution was given in [7] using state-space approach.

Although these methods have shown to be effective in removing the output envelope ripples, they result in FIR filters that have a large number of coefficients and are computationally demanding to implement on the DSP. Furthermore, the method in [6] requires special attention to numerical issues in order to achieve good results in practical application. Specifically, the solution matrix to a least-square optimization problem must first be regularized by discarding eigenvalues that are smaller than some threshold value before the solution vector is computed. In [8], a technique is presented to reduce the computational load by increasing tap spacing of the FIR filters and some encouraging results were obtained.

Recently, [9] proposed a digital compensation scheme using infinite impulse response (IIR) filters since IIR filters are known to be able to produce long impulse responses using only a small number of filter coefficients and thus will be useful in such application. These IIR filters are designed using an indirect method, where the filters are obtained from FIR filters using model reduction technique. The method involves two steps: first an FIR filter is designed using the optimization technique proposed in [6, 7]; next a low-order IIR filter is obtained using model reduction technique of [10]. This approach again requires special attention to numerical issues. Otherwise, conversion from an FIR to an IIR filter will produce inconsistent results.

In this paper, we present two state-space approaches for obtaining the digital compensation filters; one results in IIR filters; while the other in FIR filters. These compensation filters are found by minimizing the H_∞ norm of the error transfer function. Design of control system by H_∞ minimization is now a standard technique. The concept of optimal model matching by H_∞ optimization has been studied thoroughly in [11, 12, 13]. Chen and Francis [13] proposed a procedure for designing the IIR synthesis filters in multirate filter bank by converting the l_2-induced problem to one of H_∞ optimization. Here, the IIR filters are obtained directly from the solution rather than an intermediate FIR solution using the mu-analysis and synthesis toolbox in Matlab. The FIR filters, however, are obtained using the linear matrix inequality (LMI) control toolbox in Matlab.

2. DEFINING THE H_∞ CONTROL PROBLEM

Figure 2 shows a typical digital precompensation structure [6, 7]. The additional components of the digital compensation structure are the two digital filters, that is, F1 and F2. These filters are designed to precompensate for departures from a constant magnitude and phase response (in the passbands) of each of the signal reconstruction filters, LPF1 and LPF2, and to achieve gain and phase balance between these two filters. The A/D converters are used to digitize the output signal from the reconstruction filters, so that measurements can be made on the DSP system.

The aim is to find F1 and F2 such that for each of the I and Q channels, the overall discrete-time channels (from the input of the digital filter to the output of the A/D converter) has transfer function that closely approximates some

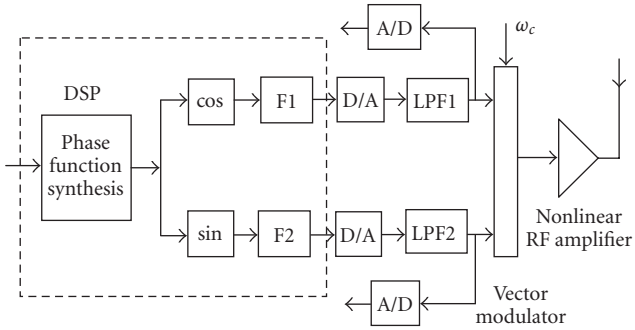

Figure 2: IQ modulator and digital precompensation structure.

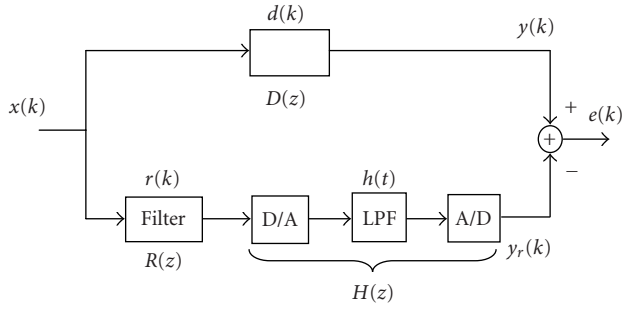

Figure 3: Generic I or Q channel optimization structure.

desired function [6, 7]. The generic I or Q channel optimization structure is shown in Figure 3.

In Figure 3, $D(z)$ is the nominal desired response, $H(z)$ is the discrete-time equivalent transfer function of the D/A analog reconstruction filter and A/D converter while $R(z)$ is the transfer function of the compensation filter. In this paper, the parameters of the analog reconstruction filter are assumed to be known *a priori* (see [6] for the identification of the analog systems parameters). Our objective is to find a stable transfer function $R(z)$ such that the cascaded system of $R(z)H(z)$ closely approximates the desired response $D(z)$ in some sense of error measure. The method proposed in [4] determines the FIR compensation filters by minimizing the least-square error, which is equivalent to minimizing the H_2 norm of the error function $\|D(z) - R(z)H(z)\|_2$. If $M(z)$ is a transfer function of a stable, causal LTI system with input $x(k)$ and output $e(k)$, then it is well known that the l_2-induced norm equals the H_∞ norm of $M(z)$ [13], that is,

$$\sup_{\|x\|_2=1} \|e\|_2 = \|M\|_\infty. \tag{1}$$

Therefore, in this paper, we propose a method for computing the FIR or IIR compensation filters via H_∞ optimization. Hence, we define the objective function as

$$J = \inf_{R(z)} \sup_{\|x\|_2=1} \|e\|_2 := \inf_{R(z)} \left\|D(z) - R(z)H(z)\right\|_\infty. \tag{2}$$

Then our precise *design problem statement* is as follows.

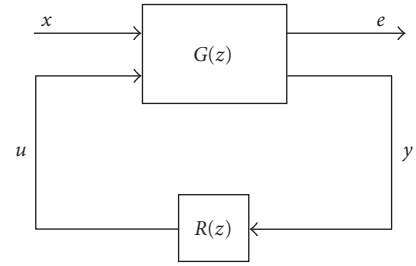

Figure 4: The standard block diagram.

Given stable FIR filters $D(z)$ and $H(z)$, find causal stable digital filter, IIR or FIR, $R(z)$ to minimize J.

This quantity J is taken to be the performance measure of the digital compensation. A small value of J means that the error $e(k)$ is uniformly small over all inputs $x(k)$. Ideally, we require $J = 0$, so that the I and Q channels are perfectly matched. This optimization is over all matrices $R(z)$ that are analytic and bounded outside the unit disc. In Sections 3 and 4, we present the state-space formulations of the digital IIR and FIR compensation filters, respectively.

3. IIR FORMULATION

In this section, we present the algorithm for finding the I and Q channel digital IIR compensation filters. This algorithm results in low-order IIR filters that are easy to implement, and are able to achieve a substantial reduction in output envelope ripples. Moreover, these IIR compensation filters are obtained directly based on systems parameters, and not via an intermediated FIR solution as was in the case of [9].

The digital IIR compensation filters are obtained using the *hinfsyn* function in Matlab, which uses the formulas described in Glover and Doyle's paper [14] for solution to the optimal H_∞ control design problem. The Matlab programs for H_∞ optimization use state-space representations of transfer functions. In this section, we present the state-space formulas relevant to the design program. Let $D(z)$ and $H(z)$ be stable systems with the following minimal realizations:

$$D(z) = \left[\begin{array}{c|c} A_D & B_D \\ \hline C_D & D_D \end{array}\right], \qquad H(z) = \left[\begin{array}{c|c} A_H & B_H \\ \hline C_H & D_H \end{array}\right]. \tag{3}$$

Since the Matlab program *hinfsyn* requires a realization in the form of Figure 4, we need to convert the generic optimization structure in Figure 3 to that in Figure 4. The *model-matching* problem in Figure 3 can be recast as a standard H_∞ control problem [12] in Figure 4 by defining

$$G(z) = \begin{bmatrix} D(z) & -I \\ H(z) & 0 \end{bmatrix}. \tag{4}$$

Then Figures 3 and 4 are equivalent.

Lemma 1. *The transfer matrix $G(z)$ has the realization*

$$G(z) = \left[\begin{array}{c|c} A_G & B_G \\ \hline C_G & D_G \end{array}\right] = \left[\begin{array}{cc|cc} A_D & 0 & B_D & 0 \\ 0 & A_H & B_H & 0 \\ \hline C_D & 0 & D_D & -I \\ 0 & C_H & D_H & 0 \end{array}\right]. \quad (5)$$

Proof. Expanding (4) gives

$$\begin{aligned} G(z) &= \begin{bmatrix} D(z) & -I \\ H(z) & 0 \end{bmatrix} \\ &= \begin{bmatrix} C_D(zI - A_D)^{-1}B_D + D_D & -I \\ C_H(zI - A_H)^{-1}B_H + D_H & 0 \end{bmatrix} \\ &= \begin{bmatrix} C_D(zI - A_D)^{-1}B_D & 0 \\ C_H(zI - A_H)^{-1}B_H & 0 \end{bmatrix} + \begin{bmatrix} D_D & -I \\ D_H & 0 \end{bmatrix} \\ &= \begin{bmatrix} C_D & 0 \\ 0 & C_H \end{bmatrix} \begin{bmatrix} zI - A_D & 0 \\ 0 & zI - A_H \end{bmatrix}^{-1} \begin{bmatrix} B_D & 0 \\ B_H & 0 \end{bmatrix} \\ &\quad + \begin{bmatrix} D_D & -I \\ D_H & 0 \end{bmatrix} \\ &= C_G(zI - A_G)^{-1}B_G + D_G, \end{aligned} \quad (6)$$

where

$$\begin{aligned} A_G &= \begin{bmatrix} A_D & 0 \\ 0 & A_H \end{bmatrix}, \qquad B_G = \begin{bmatrix} B_D & 0 \\ B_H & 0 \end{bmatrix}, \\ C_G &= \begin{bmatrix} C_D & 0 \\ 0 & C_H \end{bmatrix}, \qquad D_G = \begin{bmatrix} D_D & -I \\ D_H & 0 \end{bmatrix}. \end{aligned} \quad (7)$$

Therefore, we have the relation in (5). □

The Matlab function *hinfsyn* takes in a realization for $G(z)$ as input and outputs a realization of $R(z)$. The resulting filter $R(z)$ is an IIR filter with the same order as $G(z)$ that minimizes the H_∞ norm from x to e in Figure 4. Since *hinfsyn* works in continuous-time domain, one must perform a bilinear transformation of $G(z)$ to $G_c(s)$, then run *hinfsyn* to obtain $R_c(s)$, and then perform a bilinear transformation back to the discrete-time domain to get $R(z)$.

However, the function *hinfsyn* results in IIR filters of quite high order and are not desirable for practical implementation. It may be possible to get lower-order compensation filters if one reduces to minimal realizations at each appropriate stage, that is, if one discards uncontrollable and unobservable states. Another alternative is to reduce the order of the resulting IIR filter through model reduction techniques. There are a number of techniques available for model reduction. Some of the well-known techniques are balanced truncation [10] and optimal Hankel norm approximation [15]. In this paper, we consider the technique of balanced truncation to obtain a low-order IIR filter. The preceding results can now be summarized in the following algorithm.

Algorithm 1. *Summary of IIR Algorithm.*

(i) *Compute a state-space realization $\{A_G, B_G, C_G, D_G\}$ of the plant $G(z)$ given in* (5).
(ii) *Use bilinear transformation to transform $G(z)$ into continuous-time domain to obtain $G_c(s)$.*
(iii) *Compute $R_c(s)$ using hinfsyn function in Matlab.*
(iv) *Transform $R_c(s)$ back to discrete-time domain using bilinear transformation to get $R(z)$.*
(v) *Use model reduction techniques [10] to eliminate nearly uncontrollable or unobservable states.*

Remark 1. The two A/D converters are included in the structure such that the unknown analog filters time-domain responses $h_I(t)$ and $h_Q(t)$ can be measured using the DSP system. Note that while the A/D converters are used for the identification of the analog reconstruction filter responses, they are not in the transmission path. Therefore, it is important that these components are suitably chosen or are calibrated so that they do not introduce significant scaling or offset errors. An effective technique for compensating for the implementation errors such as gain imbalances, I and Q channel DC offset errors and phase errors, has been successfully developed in [16].

4. FIR FORMULATION

In this section, the algorithm for designing the FIR precompensation filters is presented. The digital FIR compensation filters obtained have low orders and are able to achieve significantly higher ripple reduction factor than previously existing FIR techniques [6, 7]. Here, the I and Q channel digital FIR compensation filters are found using LMI theory. In particular, the necessary state-space formulas for solving the design problem in LMI control toolbox in Matlab are derived. Consider the following lemma.

Lemma 2. *Let*

$$M(z) = \left[\begin{array}{c|c} A & B \\ \hline C & D \end{array}\right] \quad (8)$$

be stable, then $\|M(z)\|_\infty < \mu$ if and only if there is a $X > 0$ such that

$$\begin{bmatrix} A^TXA - X & A^TXB & C^T \\ B^TXA & B^TXB - I & D^T \\ C & D & -\mu^2 I \end{bmatrix} < 0. \quad (9)$$

The proof is omitted. Please see [17].

Let $D(z)$, $H(z)$, and $R(z)$ have the following minimal realizations:

$$\begin{aligned} D(z) &= \left[\begin{array}{c|c} A_D & B_D \\ \hline C_D & D_D \end{array}\right], \qquad H(z) = \left[\begin{array}{c|c} A_H & B_H \\ \hline C_H & D_H \end{array}\right], \\ R(z) &= \left[\begin{array}{c|c} A_R & B_R \\ \hline C_R & D_R \end{array}\right], \end{aligned} \quad (10)$$

where the transfer functions are defined by

$$\begin{aligned} D(z) &= C_D(zI - A_D)^{-1}B_D + D_D, \\ H(z) &= C_H(zI - A_H)^{-1}B_H + D_H, \\ R(z) &= C_R(zI - A_R)^{-1}B_R + D_R. \end{aligned} \tag{11}$$

From Sections 2 and 3, we know that the error transfer function is given by

$$E(z) = D(z) - R(z)H(z) = D(z) - H(z)R(z). \tag{12}$$

Note that the order of the transfer matrices can be interchanged because both $H(z)$ and $R(z)$ are linear time-invariant (LTI) systems. The transfer matrix $E(z)$ has a minimal realization given by

$$\left[\begin{array}{c|c} A & B \\ \hline C & D \end{array}\right] = \left[\begin{array}{ccc|c} A_H & 0 & 0 & B_H \\ B_R C_H & A_R & 0 & B_R D_H \\ 0 & 0 & A_D & B_D \\ \hline -D_R C_H & -C_R & C_D & -D_R D_H + D_D \end{array}\right]. \tag{13}$$

Expressing $R(z)$ in controllability canonical form [18] yields

$$\begin{aligned} A_R &= \begin{bmatrix} 0 & 0 & \cdots & 0 \\ 1 & 0 & \cdots & 0 \\ \vdots & & & \vdots \\ 0 & \cdots & 1 & 0 \end{bmatrix}, \qquad B_R = \begin{bmatrix} 1 \\ 0 \\ \vdots \\ 0 \end{bmatrix}, \\ C_R &= [r_1 \;\; r_2 \;\; \cdots \;\; r_{N-1}], \\ D_R &= r_0, \end{aligned} \tag{14}$$

where $r_0, r_1, \ldots, r_{N-1}$ are the impulse response of $R(z)$.

It is clear that the only unknowns in the realization in (13) are C_R and D_R. Therefore, we can use LMIs to minimize $\|D(z) - H(z)R(z)\|_\infty$.

Algorithm 2. *Summary of FIR Algorithm.*

(i) *Compute state-space matrices A and B using* (13).

(ii) *Construct the LMIs using* (9) *and solve using LMI control toolbox in Matlab.*

(iii) *Compute the FIR compensation filters using*

$$R(z) = C_R(zI - A_R)^{-1}B_R + D_R. \tag{15}$$

5. SIMULATION STUDIES

In this section, we present some simulation results to show the effectiveness of the proposed methods. The simulation studies are centred on a single channel ERMES (European Radio Message System) modulation format transmitter [6, 7]. For the results presented in Section 5.1, the two lowpass filters, LPF1 and LPF2 have a nominal 6th, order lowpass characteristic while for the results presented in Section 5.2 the analog filters have nominal 4th, order lowpass characteristic. In both sections, the analog filters have cutoff frequency of 20 kHz, but each response corresponds to particular realization of the filter circuit resulting from the perturbations of the component values about its nominal values. These analog filters are implemented using cascaded *Sallen* and *Key* 2nd-order sections where the circuit component tolerance is assumed to be 5% for resistors and 10% for capacitors. The desired response $D(z)$ is chosen to have the same magnitude characteristics as the nominal response of the reconstruction filters but constrained to have linear phase. The digital system sampling frequency is 200 kHz. In the following two sections, we present and compare some results on root mean square (RMS) envelope ripples as a measure of the modulator's performance.

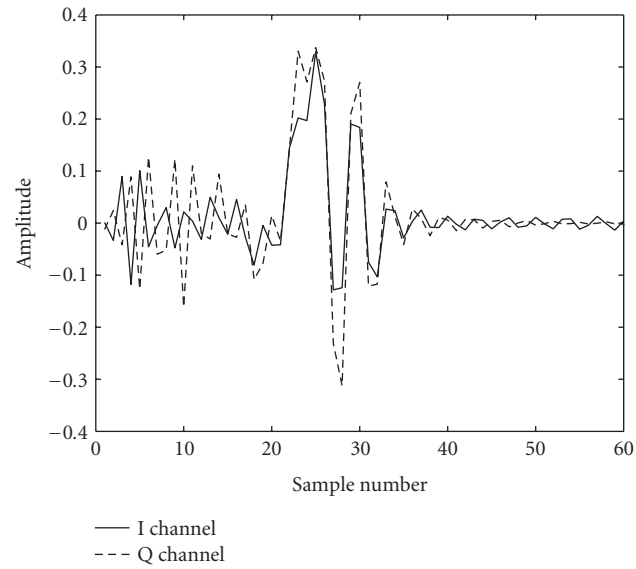

Figure 5: I and Q channel digital 20th-order IIR compensation filters impulse.

5.1. IIR compensated system

In this subsection, the simulation results of different orders of IIR compensation filters used in compensating for the shortcomings for the analog reconstruction filters are presented. Going back to the standard H_∞ control block diagram in Figure 4, the function *hinfsyn* in Matlab returns a controller $R(z)$ that has the same order as the plant $G(z)$. Based on the lengths of impulse responses chosen for $D(z)$ and $H(z)$, the realization $G(z)$ has an order of 100. Thus, the initial IIR filter obtained is of 100th order, where the numerator and denominator polynomials are 100 taps, respectively. IIR filters of this high order are not suitable for practical implementation. Therefore, model reduction techniques are employed to reduce the order of the IIR filters.

The 57th-order IIR filters are obtained by discarding the uncontrollable and unobservable states. Further reduction was carried out using model reduction technique of [10] to obtain lower-order filters. Shown in Figure 5 is an example of the impulse responses of the 20th-order IIR compensation filters. Shown in Figures 6 and 7 are the impulse responses of the 100th- and 20th-order IIR filters in both I and Q channels. To allow comparisons to be made, the impulse responses of the reduced IIR compensation filter in each

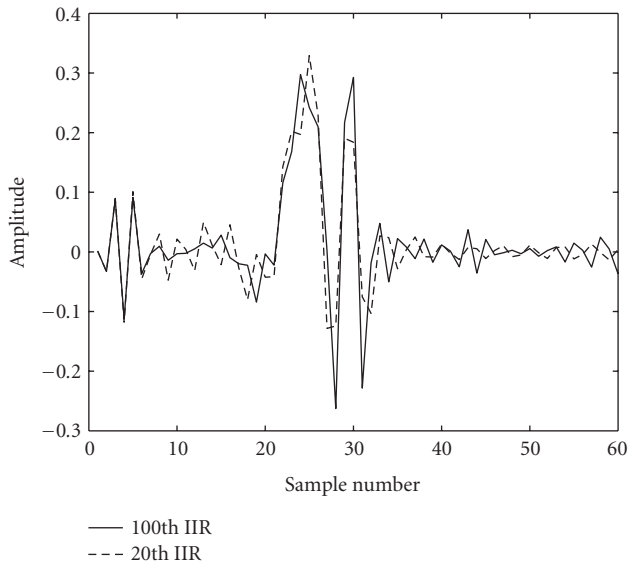

Figure 6: Plot of impulse responses of 100th-order IIR and 20th-order IIR filters in I channel.

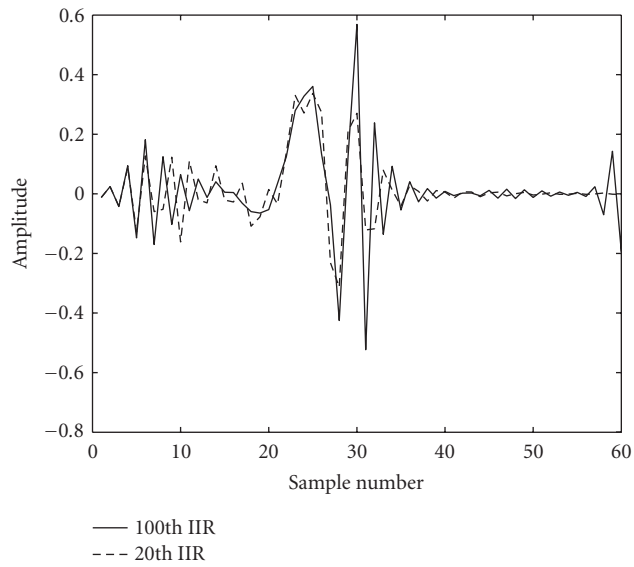

Figure 7: Plot of impulse responses of 100th-order IIR and 20th-order IIR filters in Q channel.

channel is plotted on the same graph as the original 100th-order IIR filter. This is to illustrate the effectiveness of model reduction technique in reducing the order of the IIR compensation filters. It can be seen that the impulse responses of the reduced 20th-order IIR filters approximate reasonably well the original 100th-order IIR filters.

Table 1 summarizes the RMS envelope ripples obtained using different filter order. Table 2 shows the RMS ripple values for the IIR compensated system proposed by [9]. The "ripple reduction factor" in Tables 1 and 2 are calculated as follows:

$$\text{ripple reduction factor} = \frac{\text{uncompensated RMS ripple}}{\text{compensated RMS ripple}} = \frac{3.158\,\text{mV}}{\text{compensated RMS ripple}}. \tag{16}$$

It can be seen from Table 1 that low-order IIR filters are still able to provide substantial reduction without significantly degrading the performance of the modulator. For the original 100th-order IIR filter, a reduction by a factor of approximately 54 is achieved. Since the 57th order is obtained by discarding the uncontrollable and unobservable states, no reduction in ripple reduction factor is observed.

From Tables 1 and 2, it can be seen that the new method outlined in Section 3 gives better results in terms of reducing the output envelope ripples. In addition, the technique in [9] requires special attention to numerical issues in order to get a good approximation of the original FIR filter. Therefore, it is difficult to achieve significant order reduction from FIR to IIR. Figure 8 shows the output envelope signals for the uncompensated and pre-compensated cases and it is evident that the presence of the 20th- and 15th-order IIR precompensation filters still greatly reduces the output envelope ripples.

Table 1: RMS envelope ripple for different IIR filter lengths.

IIR filter length	RMS envelope ripple (mV)	Ripple reduction factor
Uncompensated	3.158	—
100th-order IIR	0.057	54
57th-order IIR	0.057	54
20th-order IIR	0.132	24
15th-order IIR	0.137	23
10th-order IIR	0.251	13

Table 2: RMS envelope ripple for different IIR filter lengths using the method of [9].

IIR filter length	RMS envelope ripple (mV)	Ripple reduction factor
Uncompensated	3.158	—
20th-order IIR	0.146	22
18th-order IIR	0.242	13
15th-order IIR	0.246	12

5.2. FIR compensated system

Using the proposed method presented in Section 4 yields 14th- and 10th-order FIR precompensation filters. A plot of the 14th-order and 10th-order FIR compensation filters I and Q channels impulse responses is shown in Figures 9 and 10. Figure 11 shows the output envelope of the vector modulator with and without compensation. The RMS ripples recorded during the simulation studies are shown in Table 3. Table 4 shows the results obtained using the method proposed in [7].

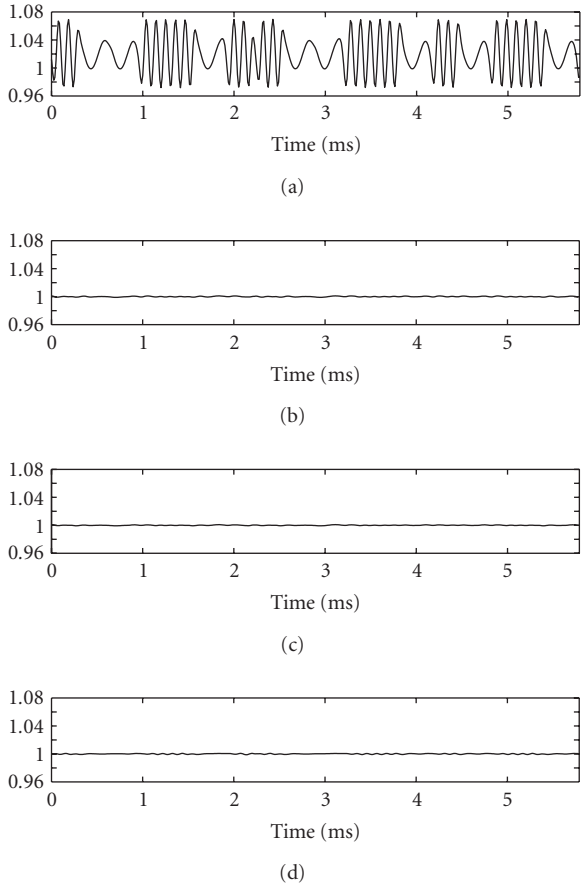

Figure 8: Envelope functions for the uncompensated and compensated modulator systems: (a) output envelope: uncompensated, (b) output envelope: compensated 100th-order IIR, (c) output envelope: compensated 20th-order IIR, and (d) output envelope: compensated 15th-order IIR.

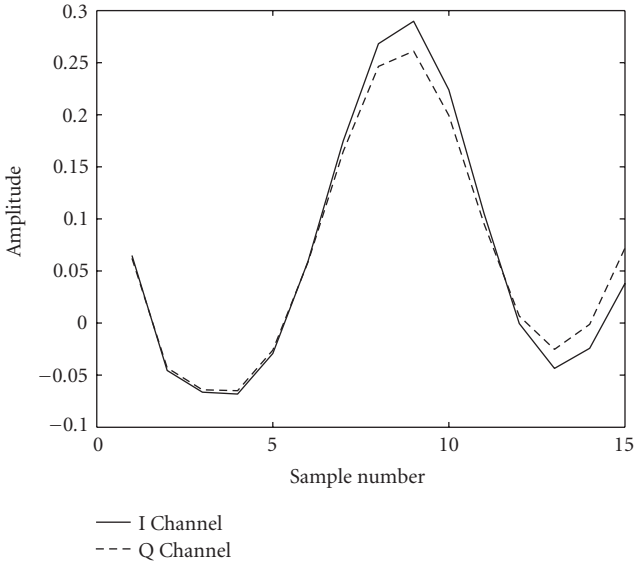

Figure 9: I and Q channel digital 14th-order FIR compensation filters impulse responses.

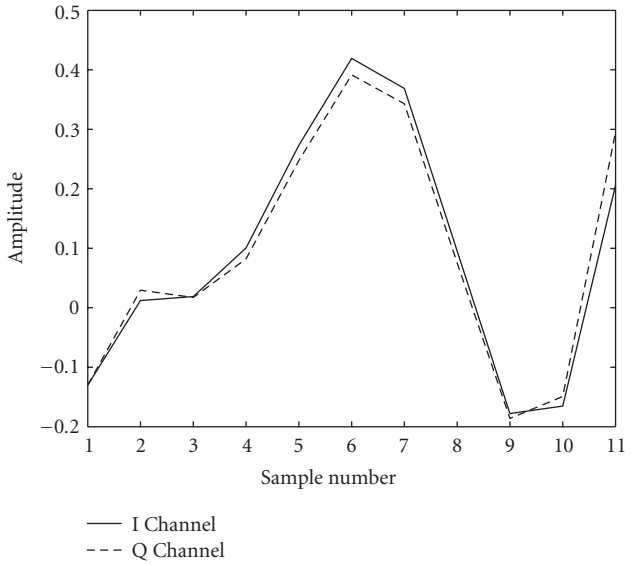

Figure 10: I and Q channel digital 10th-order FIR compensation filters impulse responses.

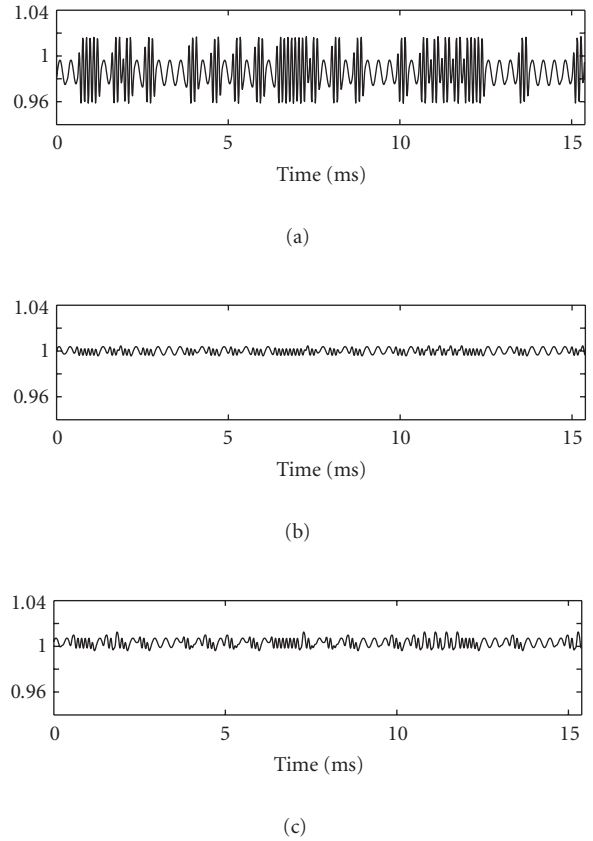

Figure 11: Output envelope ripples of the modulator for an uncompensated system, and 14th order and 10th order FIR compensated systems: (a) output envelope: uncompensated, (b) output envelope: compensated 14th-order FIR, and (c) output envelope: compensated 10th-order FIR.

Table 3: RMS envelope ripple for different FIR filter lengths.

FIR filter length	RMS envelope ripple (mV)	Ripple reduction factor
Uncompensated	1.77	—
14th-order FIR	0.25	6.9
10th-order FIR	0.45	3.9

Table 4: RMS envelope ripple for different FIR filter lengths using the method of [7].

FIR filter length	RMS envelope ripple (mV)	Ripple reduction factor
Uncompensated	1.77	—
18th-order FIR	0.28	6.3
14th-order FIR	0.74	2.4
10th-order FIR	1.52	1.1

It can be seen that the 14th- and 10th-order FIR compensation filters are able to provide substantial reduction in output envelope ripples. From the plot of envelope functions in Figure 11, the 10th-order FIR compensated system results in noticeable increase in RMS envelope ripples. Comparing the RMS ripple values in Tables 3 and 4, we can see that the new technique can achieve significantly higher ripple reduction factor than the technique of [7].

Unfortunately, simulation results for higher order of FIR filters are not presented due to the size constraint of the FIR filter. The computational burden of the LMI algorithm in Matlab increases extensively as the order of the FIR filter increases. It is anticipated that higher-order FIR compensation filters are able to provide further reduction in RMS envelope ripples thus improving the transmitted signal quality. The use of LMI techniques for designing the compensation filters is still under investigation and will be an ongoing research project. Nevertheless, it is shown that the FIR formulation using LMI techniques is indeed successful and substantial reduction in RMS envelope ripples is achieved.

6. CONCLUSION

In Sections 3 and 4, we presented two state-space solutions for finding the IIR and FIR compensation filters by solving the H_∞ optimization problem. The simulation results in Section 5 show that substantial improvements in RMS envelope ripples can be achieved using the algorithms outlined in Sections 3 and 4. These methods are simple and easy to implement using the readily available functions in Matlab, and furthermore the stability of the models is guaranteed. In addition, these methods are able to achieve significantly higher ripple reduction factor compared to the previous existing techniques.

However, there is a disadvantage in using LMI optimization due to the increase of LMI computational load with increase filter order, and thus higher-order FIR filters could not be tested. Nevertheless, research on LMI optimization is still very active and substantial speedups can be expected in the future.

ACKNOWLEDGMENT

This project was funded by the Australian Research Council (ARC) under Discovery Grant Scheme.

REFERENCES

[1] Z. Kostic and S. Seetharaman, "Digital signal processors in cellular radio communications," *IEEE Communications Magazine*, vol. 35, no. 12, pp. 22–35, 1997.

[2] T. Hentschel, M. Henker, and G. Fettweis, "The digital front-end of software radio terminals," *IEEE Personal Communications*, vol. 6, no. 4, pp. 40–46, 1999.

[3] L. Sundstrom, M. Faulkner, and M. Johansson, "Effects of reconstruction filters in digital predistortion linearizers for RF power amplifiers," *IEEE Trans. Vehicular Technology*, vol. 44, no. 1, pp. 131–139, 1995.

[4] S. Leyonhjelm and M. Faulkner, "The effect of reconstruction filters on direct upconversion in a multichannel environment," *IEEE Trans. Vehicular Technology*, vol. 44, no. 1, pp. 95–102, 1995.

[5] R. Marchesani, "Digital precompensation of imperfections in quadrature modulators," *IEEE Trans. Communications*, vol. 48, no. 4, pp. 552–556, 2000.

[6] J. D. Tuthill and A. Cantoni, "Optimum precompensation filters for IQ modulation systems," *IEEE Trans. Communications*, vol. 47, no. 10, pp. 1466–1468, 1999.

[7] A. G. Lim and V. Sreeram, "Optimum digital precompensation in IQ modulators using state-space approach," in *Proc. 5th International Conference on Optimisation: Techniques and Applications (ICOTA '01)*, vol. 1, pp. 324–331, Hong Kong, China, December 2001.

[8] G. C. Lee, J. Tuthill, and A. Cantoni, "Efficient implementation of digital compensation in IQ modulators," in *Proc. IEEE 27th International Conference on Acoustics, Speech, and Signal Processing (ICASSP '02)*, vol. 3, pp. 2697–2700, Orlando, Fla, USA, May 2002.

[9] E. H. Soh, J. Tuthill, V. Sreeram, and A. Cantoni, "Digital compensation in IQ modulators," in *Proc. IEEE Region 10 International Conference on Electrical and Electronic Technology (TENCON '01)*, vol. 1, pp. 213–218, Singapore, August 2001.

[10] B. C. Moore, "Principal component analysis in linear systems: Controllability, observability, and model reduction," *IEEE Trans. Automatic Control*, vol. 26, no. 1, pp. 17–32, 1981.

[11] M. Green and D. J. N. Limebeer, *Linear Robust Control*, Prentice Hall, Englewood Cliffs, NJ, USA, 1995.

[12] B. A. Francis, *A Course in H_∞ Control Theory*, vol. 88 of *Lecture Notes in Control and Information Sciences*, Springer-Verlag, Berlin, 1987.

[13] T. Chen and B. A. Francis, "Design of multirate filter banks by H_∞ optimization," *IEEE Trans. Signal Processing*, vol. 43, no. 12, pp. 2822–2830, 1995.

[14] K. Glover and J. C. Doyle, "State-space formulae for all stabilizing controllers that satisfy an H_∞-norm bound and relations to risk sensitivity," *Systems Control Lett.*, vol. 11, no. 3, pp. 167–172, 1988.

[15] S. Y. Kung and D. W. Lin, "Optimal Hankel-norm model reductions: Multivariable systems," *IEEE Trans. Automatic Control*, vol. 26, no. 4, pp. 832–852, 1981.

[16] Y.-H. Leung and A. Phillips, "Auto-compensation of quadrature modulators," in *Proc. 2nd Australian Workshop on Signal Processing Applications (WOSPA '97)*, pp. 19–23, Brisbane, Australia, December 1997.
[17] R. E. Skelton, T. Iwasaki, and K. Grigoriadis, *A Unified Algebraic Approach to Linear Control Design*, Taylor & Francis, London, UK, 1998.
[18] T. Kailath, *Linear Systems*, Prentice-Hall, Englewood Cliffs, NJ, USA, 1980.

A. G. K. C. Lim was born in Kuching, Sarawak, Malaysia. He received the B.S. degree with first class honours in electrical and electronic engineering from the University of Western Australia, Australia, in 2000. Currently, he is pursuing the Ph.D. degree at the University of Western Australia. His research interests include control techniques and signal processing.

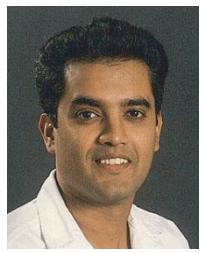

V. Sreeram obtained B.S. degree in 1981 from Bangalore University, India, the M.S. degree in 1983 from Madras University, India, and the Ph.D. degree from University of Victoria, Canada, in 1989, all in electrical engineering. He worked as a project engineer in the Indian Space Research Organisation from 1983 to 1985. He joined the Department of Electrical and Electronic Engineering, University of Western Australia, in 1990, and he is now an Associate Professor. He held visiting appointments at the Department of Systems Engineering, Australian National University, during 1994, 1995, and 1996, and at the Australian Telecommunication Research Institute, Curtin University of Technology, during 1997 and 1998. His research interests are in control and signal processing.

G. Wang obtained his B.S. and M.S. degrees from Zhejiang University, Hangzhou, and the University of Electronic Science and Technology, Chengdu, respectively. He then obtained the Ph.D. degree from the University of Western Australia, Australia, in 2001. During 1999–2002, he was a Research Associate in the Control Systems Research Group, Department of Electrical and Electronic Engineering, University of Western Australia. Since 2003, he has been an Adjunct Visiting Fellow in the same research group.